

# Origin of the Pluto–Charon system: Constraints from the New Horizons flyby



William B. McKinnon<sup>a,\*</sup>, S.A. Stern<sup>b</sup>, H.A. Weaver<sup>c</sup>, F. Nimmo<sup>d</sup>, C.J. Bierson<sup>d</sup>,  
W.M. Grundy<sup>e</sup>, J.C. Cook<sup>b</sup>, D.P. Cruikshank<sup>f</sup>, A.H. Parker<sup>b</sup>, J.M. Moore<sup>f</sup>, J.R. Spencer<sup>b</sup>,  
L.A. Young<sup>b</sup>, C.B. Olkin<sup>b</sup>, K. Ennico Smith<sup>f</sup>, the New Horizons Geology, Geophysics &  
Imaging and Composition Theme Teams

<sup>a</sup> Department of Earth and Planetary Sciences and McDonnell Center for the Space Sciences, Washington University in St. Louis, Saint Louis, MO 63130, USA

<sup>b</sup> Southwest Research Institute, Boulder, CO 80302, USA

<sup>c</sup> Johns Hopkins University Applied Physics Laboratory, Laurel, MD 20723, USA

<sup>d</sup> Department of Earth and Planetary Sciences, UC Santa Cruz, Santa Cruz, CA 95064, USA

<sup>e</sup> Lowell Observatory, Flagstaff, AZ 86001, USA

<sup>f</sup> NASA Ames Research Center, Moffett Field, CA 94035, USA

## ARTICLE INFO

### Article history:

Received 15 May 2016

Revised 7 November 2016

Accepted 11 November 2016

Available online 17 November 2016

### Keywords:

Pluto

Charon

Origin, solar system

Abundances, interiors

Pluto, satellites

Accretion

Satellites, formation

Satellites, composition

Kuiper belt

## ABSTRACT

New Horizon's accurate determination of the sizes and densities of Pluto and Charon now permit precise internal models of both bodies to be constructed. Assuming differentiated rock-ice structures, we find that Pluto is close to 2/3 solar-composition anhydrous rock by mass and Charon 3/5 solar-composition anhydrous rock by mass. Pluto and Charon are closer to each other in density than to other large ( $\geq 1000$ -km diameter) Kuiper belt bodies. Despite this, we show that neither the possible presence of an ocean under Pluto's water ice shell (and no ocean within Charon), nor enhanced porosity at depth in Charon's icy crust compared with that of Pluto, are sufficient to make Pluto and Charon's rock mass fractions match. All four small satellites (Styx, Nix, Kerberos, Hydra) appear much icier in comparison with either Pluto or Charon. In terms of a giant impact origin, both these inferences are most consistent with the relatively slow collision of partly differentiated precursor bodies (Canup, *Astrophys. J.* 141, 35, 2011). This is in turn consistent with dynamical conditions in the ancestral Kuiper belt, but implies that the impact precursors themselves accreted relatively late and slowly (to limit  $^{26}\text{Al}$  and accretional heating). The iciness of the small satellites is not consistent with direct formation of the Pluto–Charon system from a streaming instability in the solar nebula followed by prompt collapse of gravitationally bound “pebble piles,” a proposed formation mechanism for Kuiper belt binaries (Nesvorný et al., *Astron. J.* 140, 785–793, 2010). Growth of Pluto-scale bodies by accretion of pebbles in the ancestral Kuiper belt is not ruled out, however, and may be needed to prevent the precursor bodies from fully differentiating, due to buried accretional heat, prior to the Charon-forming impact.

© 2016 Elsevier Inc. All rights reserved.

## 1. Introduction

The New Horizons encounter with the Pluto–Charon system in July 2015 provided many scientific surprises (Stern et al., 2015). Foremost was the diversity, complexity, and ongoing vigor of Pluto's geology. This includes evidence for present and past glacial activity, young cryovolcanic constructs, and a most unusual solid state convective regime in a thick layer of volatile ices trapped within major structural basin (Moore et al., 2016; Grundy et al., 2016; McKinnon et al., 2016). Even Charon, half the size of Pluto,

revealed itself to have had a spectacular geologic past (Moore et al., 2016; Beyer et al., 2016).

On a more technical level, no new satellites were discovered on approach, despite four having been found in deep HST searches after the mission received its formal start (Stern et al., 2015; Weaver et al., 2016). More surprising was the discovery that Pluto's atmosphere is less distended, with an escape rate two orders of magnitude less, than had been assumed for decades – yet it is an atmosphere with extensive haze layers (Stern et al., 2015; Gladstone et al., 2016; Bagenal et al., 2016). And despite Pluto–Charon's presumed “giant impact” origin, no hint of a fossil oblateness from Pluto's or Charon's post-impact spindown or tidal evolution was detected (Moore et al. 2016; Nimmo et al., 2017).

\* Corresponding author.

E-mail address: [mckinnon@wustl.edu](mailto:mckinnon@wustl.edu) (W.B. McKinnon).

This paper is focused on origins issues for the Pluto–Charon system, and indeed on how what we have learned from New Horizons illuminates our understanding of the evolution of the entire Kuiper belt. The orbital architecture of the Kuiper belt all but demands an epoch of planetary migration and dynamical instability. The most developed and certainly best known model for this migration and instability, the Nice model, posits a compact giant planet configuration and a massive outer disk of remnant planetesimals (e.g., Tsiganis et al., 2005; Levison et al., 2008, 2011; Morbidelli et al., 2008). The Nice dynamical instability implants Neptune within the disk, where its orbit circularizes as the ice giant migrates outward. In doing so, Neptune scatters planetesimals from the disk into the present range of the Kuiper belt and beyond, and the surviving planetesimals (both resonant and non-resonant) are trapped. Pluto is one of these (resonant) bodies, and the Nice model, in its original schema, predicts Pluto originally accreted well inside its present position, somewhere in the 20-to-34 AU range (Levison et al., 2008, 2011).

More recent work has evolved along a related but different avenue. The giant planets still form in a compact configuration in the solar nebula, but now there is at least one additional ice giant in the system (Nesvorný and Morbidelli, 2012). After nebula dispersal, there is a prolonged evolution of Jupiter, Saturn, and the ice giants, followed by a dynamical instability that results in ejection of the extraneous ice giant(s), and after which Neptune follows a much slower evolution outward through a depleted planetesimal belt. In this post-Nice conception, not only is the present-day orbital configuration of Jupiter, Saturn, Uranus, and Neptune explainable (Nesvorný and Morbidelli, 2012), but the observed orbital properties of the major Kuiper belt reservoirs (e.g., the hot classicals, the resonant populations, and the cold classicals) can be matched as well (Nesvorný, 2015a,b; Nesvorný and Vokrouhlický, 2016).

Notably, the initial massive planetesimal disk in these new migration/instability models extends from roughly 24 AU to 30 AU, and likely originally contained thousands of Pluto-scale bodies (Nesvorný and Vokrouhlický, 2016), while a low-mass extension of this ancestral Kuiper belt stretched from 30 AU out to at least 40 AU. In the original Nice model, one goal was to find initial conditions or parameters to sufficiently delay the instability amongst the major planets so as to plausibly explain the Late Heavy Bombardment on the Moon, circa 3.9 GYA (Gomes et al., 2005). In the newer work, the instability occurs early, generally in well under 100 million years after solar nebula dispersal (Nesvorný and Morbidelli, 2012; Nesvorný and Vokrouhlický, 2016).

So, do New Horizons results inform or constrain such migration/instability models, or the timing of the dynamical instability? Is the Nice model in its original form or that proposed by Nesvorný and Morbidelli (2012) consistent with the formation of the Pluto–Charon binary? And is a giant impact still implicated, and if so, when did it likely occur? Or could the Pluto–Charon system have formed by a different mechanism? In this paper we address these questions, using the data returned from the New Horizons encounter. We focus on the compositions of Pluto, Charon, and the four smaller moons, and how these constrain their origin.

## 2. Bulk composition

In terms of composition, extensive studies of comets, asteroids, meteorites (especially the more recent falls Tagish Lake and Sutter's Mill), interstellar dust particles (IDPs), interstellar molecular clouds, and star-forming regions support the concept that the planetesimal disk that birthed Pluto and other Kuiper belt objects (KBOs) was composed of subequal amounts of volatile ices (including volatile organics), less volatile carbonaceous matter, and refractory "rock" (e.g., references in Festou et al., 2004; McKinnon et al., 2008; Kofman et al., 2015). Volatile ice compositions are best

represented by cometary comae (Bockelée-Morvan et al., 2004; Crovisier et al., 2009; Mumma and Charnley, 2011), but differences may exist among cometary dynamical classes (Fink, 2009; Hartogh et al., 2011; A' Hearn et al., 2012). Macromolecular carbonaceous compounds (CHON) were seen at Halley (Jessberger et al., 1988; Fomenkova, 1999), were analyzed in Stardust samples (Sandford et al., 2006; Brownlee, 2014), inferred from infrared emission spectra of several comets (e.g., Lisse et al., 2007), inferred from Rosetta VIRTIS infrared spectra of comet 67P/Churyumov–Gerasimenko (Capaccioni et al., 2015), and were sampled directly by the Philae lander during its brief operation at the surface of comet 67P/Ch-G (Goesmann et al., 2015).

The rock component is no doubt multicomponent (Brownlee, 2014), but can be usefully compared with the most primitive carbonaceous chondrites, as exemplified by Tagish Lake: a fine-grained, opaque matrix of phyllosilicates, sulfides, and magnetite, surrounding aggregates of olivine, pyroxene and other minerals and inclusions (some high temperature), and showing evidence for pervasive but incomplete low-temperature, aqueous alteration (Brown et al., 2001; Zolensky et al., 2002). This is not to suggest that Tagish Lake is a precise mineralogical model for cometary rock or rock within Pluto, but (1) such rock should be solar in composition or close to it (with respect to elements other than H, C, O, N, and noble gases) and (2) as planetesimals accreted and evolved between ~20- and 34 AU, various degrees of aqueous alteration likely occurred prior to final incorporation into Pluto.

## 3. Bulk properties of Pluto and Charon

### 3.1. Results from New Horizons

Whole disk imaging from New Horizons (Stern et al., 2015; Nimmo et al., 2017), and determination of the system barycenter from ground- and HST-based astrometry and mutual event lightcurves (Brozović et al., 2015), have provided firm size and density constraints for Pluto and Charon. Pluto and Charon's mean radii are  $1188.3 \pm 1.6$  km and  $606.0 \pm 1.0$  km, respectively ( $2\text{-}\sigma$ ). The corresponding bulk densities are  $1854 \pm 6$  kg m<sup>-3</sup> and  $1702 \pm 17$  kg m<sup>-3</sup> ( $1\text{-}\sigma$ ) (Nimmo et al., 2017). Pluto and Charon have rather similar bulk densities (to within 10%), more similar to each other than to almost all other large ( $\geq 1000$ -km diameter) bodies in the Kuiper belt (Fig. 1), especially Eris and Haumea (Quaoar's density is presently uncertain).

The question then arises whether the modest difference between Pluto and Charon is physically meaningful or whether it is simply a property of the internal structures of the respective bodies (e.g., the higher pressures within Pluto).

We address this question through simple structural models. Fig. 2 illustrates representative internal structures for Pluto and Charon, based on the radii and densities above and the assumption of hydrostatic equilibrium. The internal structure assumed for both, for simplicity, is that of a hydrated rock core and an overlying ice mantle, with the goal being to quantify the rock/ice ratios of the two bodies. We do not know for certain that Pluto and Charon are fully differentiated, but all the geological inferences in Stern et al. (2015) and Moore et al. (2016) point in that direction. There is certainly no hint that they are undifferentiated ice-rock mixtures. For example, if either were undifferentiated, we would expect increasing amounts of ice II to form at depth as the bodies cooled over geologic time, which would lead to a global volume decrease and strong surface compression and compressional tectonics (thrust faults) (McKinnon et al., 1997). This is not seen; rather, the tectonic evidence is exactly the opposite – for global extension (Stern et al., 2015; Moore et al., 2016; Beyer et al., 2016).

We note that at the velocity and distance of the 2015 flyby (Stern et al., 2015) it was not possible to measure or constrain

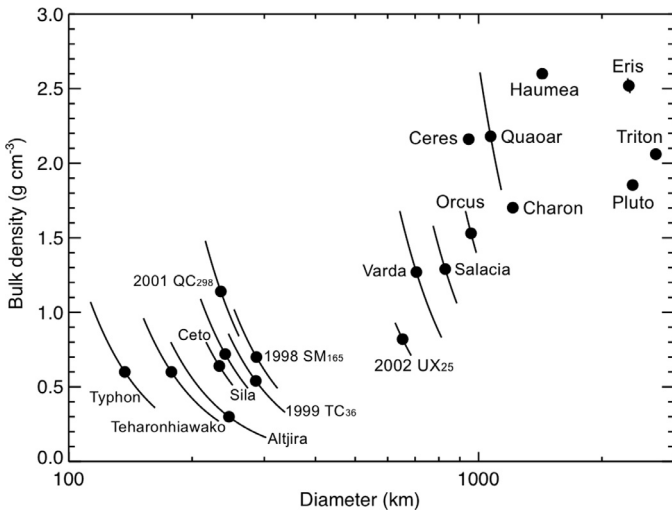


**Fig. 1.** Densities of large and midsize Kuiper belt objects and related bodies (Centaur, Ceres), after Grundy et al. (2015); cf. Brown et al. (2013). Pluto and Charon are more similar to each other than to Triton or the dwarf planets Eris and Haumea. The difference in density between Pluto and Triton can be partly or largely explained by the presence of high-pressure ice phases or a deep dense ocean within Triton (McKinnon et al., 1997; Hussmann et al., 2006), but Eris and Haumea are definitely much more rock-rich (see text). The sizes and densities of Eris and Haumea are from Sicardy et al. (2011) and Lockwood et al. (2014), respectively; for other than Pluto and Haumea, densities for the primary of a given binary pair are calculated from Kepler's 3rd Law assuming the same density and albedo for both primary and secondary.

the degree-2 gravity field of either Pluto or Charon, so we cannot use such measurements to infer their moments-of-inertia. The shapes of both are spherical to within 0.6% (Pluto) or 0.5% (Charon) (Nimmo et al., 2017), which are consistent with either differentiated or undifferentiated interiors, if the shapes are hydrostatic (McKinnon et al., 2014). This does not mean that Pluto and Charon have no fossil rotational or tidal oblateness, only that to the precision of New Horizons imagery and occultation measurements we cannot detect such.

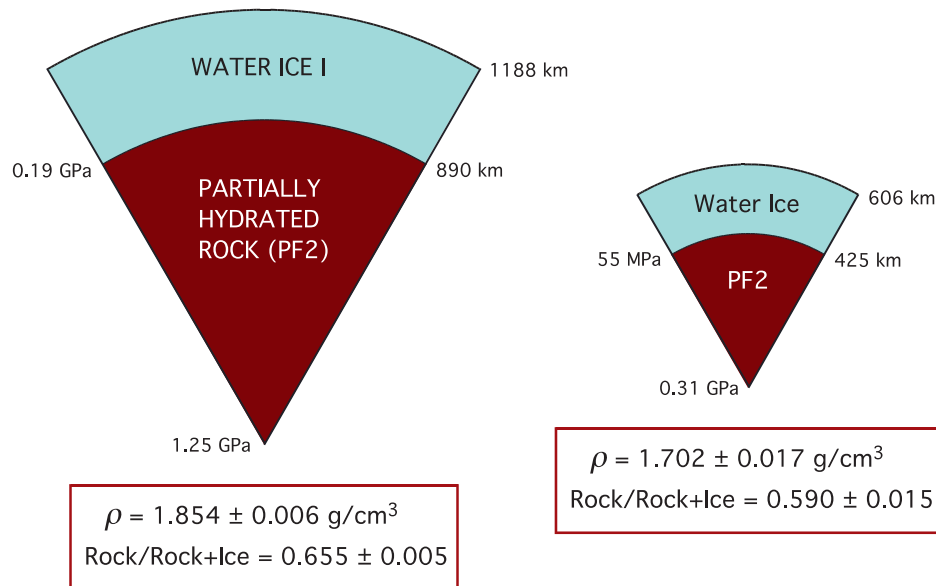


**Fig. 2.** Simple structural models of Pluto and Charon, calculated with ICYMOON (Mueller and McKinnon, 1988). Densities for Pluto and Charon are from Nimmo et al. (2017) and that for solar-composition rock are updated from Mueller and McKinnon (1988); see text. Rock mass fractions are calculated on an anhydrous basis and rounded to the nearest 0.5%, with uncertainties rounded up from  $1\sigma$  to account for systematic uncertainties in the radius determinations as well as a range of possible internal temperature structures. The larger uncertainty for Charon is due to the relative uncertainty in its mass. In these models, temperature profiles are assumed conductive, with heat flows increased by 50% (Pluto) and 25% (Charon) over present-day, steady state radiogenic levels (McKinnon et al., 1997); temperatures at the base of Pluto's ice shell are limited to 250 K, emulating solid state convection.

**Table 1**

Mineral components of carbonaceous rock types (in  $\text{g kg}^{-1}$ ), with associated STP densities.

|                        | PF rock <sup>a</sup> | PF2 rock <sup>b</sup> | $\rho_0^c$ ( $\text{g cm}^{-3}$ ) |
|------------------------|----------------------|-----------------------|-----------------------------------|
| Anorthite              | 16                   | 18.8                  | 2.760                             |
| Antigorite             | 457                  | 535.0                 | 2.665 <sup>d</sup>                |
| Magnetite              | 111                  | 102.3                 | 5.200                             |
| Millerite              | 26                   | 22.1                  | 5.374                             |
| Nepheline              |                      | 41.6                  | 2.640                             |
| Orthoclase             | 31                   |                       | 2.623                             |
| Tremolite              | 134                  | 102.5                 | 2.964                             |
| Troilite               | 225                  | 177.7                 | 4.850 <sup>e</sup>                |
| $\langle \rho \rangle$ | <b>3.26</b>          | <b>3.14</b>           |                                   |

<sup>a</sup> Mueller and McKinnon (1988).

<sup>b</sup> Updated using abundances in Lodders (2003).

<sup>c</sup> From mindat.org, except where indicated.

<sup>d</sup> Calculated from  $2.520 \text{ g cm}^{-3}$  Mg-endmember and  $\text{Mg\#} = 83.2$ .

<sup>e</sup> Anthony et al. (1990).

The rock mineralogy chosen for the cores in Fig. 2 is based on the thermochemical equilibrium calculations of Prinn and Fegley (1981) for rock condensed in the protojovian nebula. Although our ideas of satellite origin have evolved considerably since that paper, the Prinn and Fegley (1981) rock model has the virtue of being hydrated and oxidized, and solar in composition. Alternative rock models are discussed at the end of this section.

The rock in Prinn and Fegley (1981), which included silicates, oxides (magnetite) and sulfides (troilite and millerite), was modeled in Mueller and McKinnon (1988) as “PF rock”. Since that latter paper, solar abundances have been updated and revised numerous times (e.g., Anders and Grevesse, 1989; Lodders, 2003; Asplund et al., 2009; Lodders et al., 2009; Palme et al., 2014). We have opted to update the PF-rock mineralogy with the recommended abundances from Lodders (2003), as in some recent icy satellite models (McKinnon and Bland, 2011), and this updated mineralogy is given in Table 1 as “PF2 rock”. The most important changes are to the magnesium, iron, and sulfur abundances (decreased by 5%, 7% and 13%, respectively, with respect to Si, when compared with those in, e.g., Anders and Ebihara (1982)). Subsequent revisions to the

abundances of these important rock-forming elements have been very small (Appendix), and we further note that the original calculations in Prinn and Fegley (1981) were based on even earlier abundance tables. The overall effect on the mean rock density (PF2 vs. PF) is at the several percent level.

The STP density of this modeled rock is  $3140 \text{ kg m}^{-3}$ , which is notably more than that of typical hydrated (CI and CM) carbonaceous chondrites, when porosity is taken into account (their grain densities are  $\sim 2400$ -to- $3000 \text{ kg m}^{-3}$ ; Britt and Consolmagno, 2000; Consolmagno et al., 2008; Macke et al., 2011). In bulk, the porosities of CI and CM meteorites are generally quite high ( $>20\%$ ; Consolmagno et al., 2008; Macke et al., 2011); moreover, they contain bound water, carbonates, hydrated sulfate salts (some of possible terrestrial origin; Gounelle and Zolensky, 2001; Airieau et al., 2005), and of course, carbonaceous matter. In terms of interior models, porosity should not persist at the pressures pertinent to Pluto's core, though some porosity probably cannot be ruled out for Charon's core (Malamud and Prialnik, 2015; and see discussion in Zolotov (2009)). Likewise, hydrated sulfates and bound (as opposed to structural) water should not be stable at the several 100 MPa level and thermal conditions in the rock core of Pluto (see Mueller and McKinnon (1988)). Thus we retain the use of PF2 rock as reasonable average rock model for Pluto and Charon, at least for the purposes of this paper.

Doing so, we find that Pluto and Charon's rock/ice mass ratios are indeed similar (Fig. 2), with Pluto being about 2/3 rock by mass and Charon about 60% rock by mass. Charon is nominally icier, by about 10%, and the difference appears statistically significant, even at the  $3\sigma$  level. Note that PF2 rock is 6.8%  $\text{H}_2\text{O}$  by mass, and the rock mass fractions in Fig. 2 have this water counted in the ice mass fraction. The models in Fig. 2 are designed to constrain bulk ice/rock ratios taking into account temperature and pressure effects, but they do not incorporate such plausible details as internal oceans (e.g., Hussmann et al., 2006; Robuchon and Nimmo, 2011), carbonaceous layers (McKinnon et al., 1997), crustal porosity (e.g., Besserer et al., 2013), or surface volatile ice layers (McKinnon and Mueller, 1988). Such details are important, e.g., if Pluto has an ocean while Charon does not, then the inferred rock/ice ratios of both bodies would be more similar (that is, water is denser than ice, so Pluto would need less rock to match its bulk density). Such considerations are also important because Charon's iciness compared with that of Pluto is a major constraint on Charon-forming impact models (Canup, 2005, 2011; Desch, 2015).

We address these details through some simple calculations. The mean density of either body,  $\langle\rho\rangle$ , is given by  $(m_s/\rho_s + m_i/\rho_i)^{-1}$ , where  $m_s$  and  $m_i$  are the rock and ice mass fractions, respectively, and  $\rho_s$  and  $\rho_i$  are the mean density of the rock core and ice mantle, respectively. This can be inverted to give  $m_s$  as a function of variable  $\rho_i$  with  $\langle\rho\rangle$  and  $\rho_s$  fixed. Fig. 3 shows the variation in Pluto's  $m_s$  as a function of increasing  $\rho_i$  from its mantle average in the ICYMOON calculation in Fig. 2. Thus, if Pluto's effective  $\rho_i$  increases because there is a deep ocean (and if no such ocean exists on Charon), Fig. 3 shows the necessary increase in the average  $\rho_i$  for the  $m_s$  values of Pluto and Charon to be considered the same. Fig. 3 shows that the required increase in  $\rho_i$  is  $\sim 100 \text{ kg/m}^3$ , equivalent to melting the entire ice mantle, which is clearly inconsistent with Pluto's rugged geology (Stern et al., 2015).

Now, this does not mean Pluto does not have an internal ocean. In the absence of solid state convection in the water ice mantle, the melting temperature is reached conductively for present-day, steady state, chondritic (U, Th,  $^{40}\text{K}$ ) radiogenic heat flow conditions at depths of  $>250 \text{ km}$  (Hussmann et al., 2006; Moore et al., 2015). For higher heat flows (from stored core heat) the ice shell should be somewhat thinner (Robuchon and Nimmo, 2011; Hammond et al., 2016), and if the ocean contains salts, ammonia, or methanol (all of which lower the water-ice melting temperature),

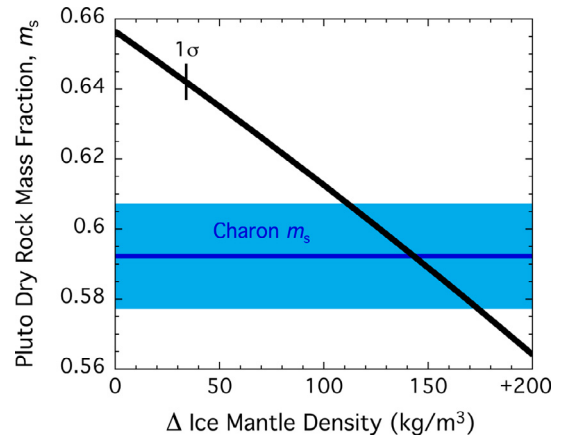


Fig. 3. Decreasing Pluto's rock mass fraction  $m_s$  as a function of effectively boosting its ice mantle density via ocean formation. The mass fractions of both bodies can be considered the same to within  $1\sigma$  if the ice mantle density increases by  $\sim 100 \text{ kg/m}^3$ . This is equivalent to melting Pluto's entire ice shell, an unlikely scenario.

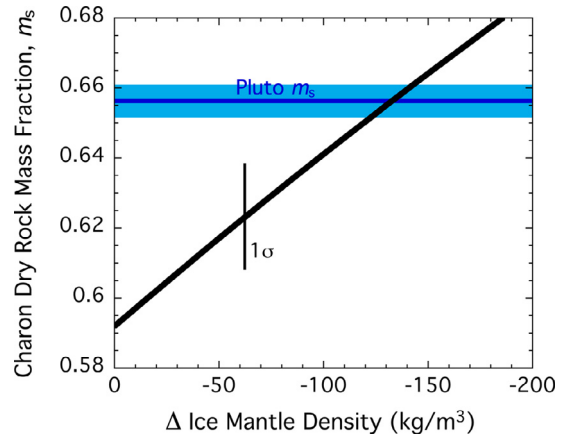


Fig. 4. Increasing Charon's rock mass fraction  $m_s$  as a function of effectively reducing its ice mantle density via porosity. The mass fractions of both bodies can be considered the same to within  $1\sigma$  if the ice mantle density decreases by  $\sim 90 \text{ kg/m}^3$ . This is equivalent to 10% porosity throughout Charon's ice mantle.

the ocean today should be thicker and the ice shell thinner still (Hussmann et al., 2006). In contrast, it is very difficult for Charon to retain enough internal radiogenic heat to maintain an internal ocean today (see Fig. 11 in McKinnon et al., 2008). Stern et al. (2015) and Moore et al. (2016) cite the spectacular extensional rifting of Charon's surface as circumstantial evidence for the freezing of such an ocean, and Beyer et al. (2016) provide quantitative estimates of the required positive volume change (about 1.5%) to account for Charon's surface extension, which is easily accommodated through freezing of an  $\sim 30$ -km thick, ancient ocean.

The same approach as above can be used to examine the role of porosity in Charon's ice mantle. Adopting the end member possibility that Pluto's water-ice bedrock and mantle have no porosity, we can ask how much does Charon's ice mantle density need to be lowered (meaning how much porosity is necessary) for its  $m_s$  to increase to match Pluto's. This is illustrated in Fig. 4, which shows that a similar change in  $\rho_i$  is necessary as in Fig. 3, but in the opposite direction. In this case, however, a decrease in  $\rho_i$  by  $90 \text{ kg/m}^3$ , or equivalently, 10% porosity mantle-wide, or 20% porosity in the outer 75 km, is at least conceivable.

GRAIL gravity results have shown that the upper few kilometers of the lunar highlands crust have an average porosity of about 12%, with some regions or areas likely having porosity extend to much greater depths (Wieczorek et al., 2013). On the Moon, such

porosity is thought to be due to the accumulated effects of the Late Heavy Bombardment. Charon's surface is similarly old, with portions heavily cratered and other portions heavily tectonically disrupted (Stern et al., 2015; Moore et al., 2016; Beyer et al., 2016), so such levels of porosity are not implausible, and are sustainable at least in the near-surface under modest pressures and present-day, cool thermal conditions (Durham et al., 2005). The more pertinent question is whether such porosity is sustainable at greater depths and during the greater heat flow conditions of the distant past, when Charon was tectonically and cryovolcanically active (Moore et al., 2016). Detailed analysis so far (Bierson et al., 2016 and in prep.) suggests that the answer is probably not, especially as Pluto's icy bedrock will have porosity as well. We conclude that Charon is indeed icier than Pluto.

The inference for an icier Pluto is reinforced when we consider the amounts of surficial volatile ices on Pluto ( $N_2$ ,  $CH_4$ , and  $CO$ ; Grundy et al., 2016), but absent on Charon, and which are apparently greater than a kilometer thick in places (the north polar terrain, Lowell Regio; Sputnik Planitia; these names being informal). A few kilometers, globally averaged, of all of these volatile ices could raise Pluto's  $m_s$  estimate by  $\sim 0.5\%$ , or about one standard deviation (McKinnon et al., 1997). That is, removing surface volatile ices from the mass balance consideration implies a denser, and hence more rock-rich, bulk interior.

### 3.2. Alternative rock mineralogies

Within the paradigm of solar composition rock, one can of course choose greater (or lesser) levels of hydration (technically, hydroxylation), oxidation, and even carbonation than that shown in Table 1. Similar arguments and a similar logical path to that just presented can be followed. Absolute rock mass fractions will change, but on an anhydrous and carbon-free basis, rock mass fractions will change much less. And the implications derived from comparing relative abundances should be similar overall. Only if one adopts an extreme mineralogical model, such as in Zolotov (2009), which all but eliminates the need for a separate water-ice phase, would our internal picture of Pluto, Charon, and other large KBOs change drastically. We opt to not pursue the latter path in this paper.

### 3.3. Results from Rosetta

Our Pluto and Charon mass fractions can also be usefully compared with estimates of cometary composition from recent spacecraft missions. Although the bulk densities of comets are now recognized as quite low (well under  $1000\text{ kg/m}^3$ ; e.g., Kofman et al., 2015; Davidsson et al., 2016), dust-to-gas ratios may be quite high. The latter have been measured for both 9P/Tempel 1, during the Deep Impact experiment (Küppers et al., 2005), and for 67P/Churyumov-Gerasimenko by Rosetta during its long orbital embrace (Rotundi et al., 2015). Both of these comets are Jupiter-family, and are presumably derived from the scattered (or scattering) disk, which means they formed or accreted in the same region of the outer Solar System as Pluto: the ancestral Kuiper belt.

The wealth of measurements at 67P/Ch-G are particularly instructive, and have been used to estimate the primordial compact, or grain, density of that comet. Davidsson et al. (2016) propose, in their model "composition A," that 67P/Ch-G is 25% metal/sulfides, 42% rock/organics, and 32% ice by mass. For their assumed component densities, the overall grain density is  $1820\text{ kg/m}^3$ . A somewhat more detailed model by Fulle et al. (2016) posits  $5 \pm 2$  volume % Fe-sulfides of density  $4600\text{ kg/m}^3$ ,  $28 \pm 5\%$  Mg,Fe-olivines and -pyroxenes of density  $3200\text{ kg/m}^3$ ,  $52 \pm 12\%$  hydrocarbons of density  $1200\text{ kg/m}^3$ , and  $15 \pm 6\%$  ices of density  $917\text{ kg/m}^3$ . This composition yields a primordial grain density (dust+ice) of

$1885 \pm 240\text{ kg/m}^3$ . Both of these density estimates are consistent with Pluto-Charon, especially as Pluto's uncompressed (STP) density (from the model in Fig. 2) is close to  $1820\text{ kg/m}^3$  and that of the system as a whole is close to  $1800\text{ kg/m}^3$ .

The potential compositional and structural implications of these proposed 67P/Ch-G compositions, when applied to Pluto and Charon, are fascinating. The amount of ice in the Davidsson et al. (2016) composition is a good match to our Pluto models. Their rock/organics component, however, is taken to be half graphite ( $2000\text{ kg/m}^3$ ) by volume. The Fulle et al. (2016) composition is more divergent. It is very ice poor, and is on the order of 50% light hydrocarbons by volume. The possibility of massive internal graphite or carbonaceous layers within Pluto was discussed in McKinnon et al. (1997), but then as now it is difficult to confirm or deny that such layers exist, within Pluto or other large KBOs.

The specific bulk cometary compositions advocated in Davidsson et al. (2016) and Fulle et al. (2016) are far from definitive. That is, they differ from each other (and is the gas-to-dust ratio of an outgassing body actually representative of its interior composition?), but the importance of carbonaceous, CHON-like material to the makeup of comets seems undeniable (e.g., Fomenkova, 1999; Fray et al., 2016). For Pluto, Charon, and other large Kuiper belt worlds, it remains an important "known unknown" with respect to their internal structures and evolutions.

## 4. Kuiper belt density trends

The preceding section does not specifically address the larger issue of the size-density trend for the Kuiper belt as whole (Fig. 1). Including Triton, we can say that dwarf planets of the Kuiper belt, if sufficiently large and/or warm, can have deep, dense oceans or internal layers of dense, high pressure ice phases, all of which serve to lower the inferred rock/ice ratio from what might be simply assumed from bulk density alone. Triton is in this category, but even so, its rock mass fraction is likely only greater than that of Pluto by about 0.05 (based on structural calculations in McKinnon et al. (1997)), about the same difference ( $\Delta m_s$ ) as between Pluto and Charon. One can hypothesize physical effects due to Triton's capture by Neptune, its tidal circularization, and cannibalism of preexisting Neptune satellites, all of which could alter its bulk composition and density (McKinnon et al., 1995). But the rock/ice ratios of the Triton and the Pluto system are closer than they might seem initially from Fig. 1.

Haumea and Eris are smaller and substantially denser than Triton, and if differentiated, their internal pressures and temperatures preclude high-pressure ice layers and all but thin oceans maintained by antifreezes such as ammonia (and even in this case, for Eris only). The canonical explanation given for Haumea's high density (with respect to that of Pluto) is that a "giant impact" stripped it of much of icy mantle, set it rapidly spinning, and yielded an extended dynamical family of very water-ice-rich bodies (as well as ice-rich moons) (Brown, 2008). Barr and Schwamb (2016) offer that Eris also suffered a mantle stripping collision, though independent evidence of such an impact is lacking.

What can be stated is that the trend from very underdense smaller KBOs to very dense dwarf planets in Fig. 1 cannot be simply explained by pore collapse under pressure of otherwise uniform composition worlds (McKinnon et al., 2008; Brown, 2013). If the impact stripping explanation can be generalized, then large differentiated KBOs would tend to evolve to be more rock-rich, while any ejected icy fragments would tend to make the smaller and midsize KBO population, over time, more ice-rich as a whole (but without necessarily making their surfaces obviously icy in the manner of the Haumea dynamical family), perhaps explaining the trend. Brown (2012) outlined a simple, heuristic model of this process, but concluded that the ice/rock fractionation process

was too inefficient to explain such observations as in Fig. 1. Large impacts do, however, offer a natural pathway to generate stochastic density and compositional variations among the largest (i.e., differentiated) KBOs: the dwarf planets (Barr and Schwamb, 2016).

## 5. Pluto's small satellites

The small satellites, Styx, Nix, Kerberos, and Hydra, have an icier surface appearance than Pluto or Charon. All have geometric albedos in excess of 50%, with that of Hydra possibly near 85% (Weaver et al., 2016). If the satellites are rubble piles, which is likely given their irregular shapes, small sizes, impact crater densities (Weaver et al., 2016) and plausible collisional histories (Walsh and Levison, 2015), impacts with small Kuiper belt (i.e., heliocentric) objects will occur in the gravity regime: most ejecta will be low-velocity and local (Housen and Holsapple, 2011). Thus, surface composition should be more or less indicative of bulk composition, which we infer to be quite icy on the basis of their high albedos. Moreover, recently returned New Horizons LEISA spectra (Reuter et al., 2008) for Nix and Hydra confirm the presence of water ice, and possibly, ammonia ice in some form, on their surfaces (Cook et al., 2016). The iciness of the small satellites and their coplanar, prograde orbits are hallmarks of an origin as regular satellites of Pluto–Charon (Stern et al., 2006; Canup, 2011). Captured KBOs of that size (~10–50 km across) would have much lower albedos due to a much more primitive composition, and not follow such regular orbits.

We note that mass estimates from astrometry are not yet precise enough to yield meaningful density constraints for the small satellites (Brozović et al., 2015),<sup>1</sup> but future improvements to the astrometric solutions will very likely provide cosmogonically useful density constraints for the largest of the small satellites, Nix and Hydra.

## 6. Implications for origins

### 6.1. Giant impact

The leading model for the formation of the Pluto–Charon binary is that of giant impact (McKinnon, 1984, 1989; Canup, 2005, 2011). The relative rock fractions within Pluto and Charon do not in themselves support or rule out the impact model, but do constrain the parameters of the impact (the iciness and differentiation state of each precursor body, impact parameter [or degree of grazing], and relative velocity at distance,  $v_\infty$ ). For example, if the two precursor bodies were undifferentiated *and of the same or similar composition*, and suffered a grazing impact, we would not expect different rock mass fractions for Pluto and Charon; moreover, we would definitely not expect a family of small icy satellites, and such an impact scenario is, dynamically, a poor candidate for generating disk of material from which small satellites can form regardless (Canup, 2011).

Conversely, Pluto and Charon may have formed from the collision of two fully differentiated precursors, precursor bodies that could have different rock mass fractions due to their different collisional histories (e.g., Brown, 2012; Barr and Schwamb, 2016). Numerical simulations show that in this situation an icy debris disk can form from which the small satellites could potentially accrete (Canup, 2011), but Charon in such simulations ends up much icier

than Pluto (in a manner similar to a rock-rich Moon forming via a giant impact on the differentiated proto-Earth). Of all the numerical models published to date, a somewhat icier Charon and ice-dominated small satellites are most consistent with the collision of (only) partially differentiated precursor bodies, with surface ice layers between 10–15% of the total mass of each (Canup, 2011).

The numerical simulations of Canup (2011) also imply that the precursor bodies in the great collision must approach each other with a relatively low  $v_\infty$ , less than about 0.7 km/s. This is in turn consistent with conditions in the ancestral Kuiper belt (the remnant planetesimal disk referred to in Sec. 1) (Levison et al., 2011; Johansen et al., 2015), but such low  $v_\infty$  are not obviously consistent with the very dynamically excited environment of the Nice instability. Such low approach speeds (implying impact speeds  $\leq 1.4$  km/s) are also generally inconsistent with the dynamical environment of Pluto's past or present 3:2 resonant orbit with Neptune, though certain interacting subpopulations do have appropriate low-velocity tails (i.e., the plutinos and the so-called "hot classicals"; see Fig. 3 in Greenstreet et al., 2015).

Desch (2015) has proposed that a relatively rock-rich Charon can form in a giant impact between differentiated precursors as long as each precursor retains a primordial, rock-ice crust. In this model enough of this primordial rock-ice ends up in orbit to build a Charon of the appropriate composition. The model was fine-tuned to yield a (somewhat underdense) Charon of 1630 kg/m<sup>3</sup>. If primordial impactor densities of 1835 kg/m<sup>3</sup> (the present system average) are assumed, the nominal model (Table 3 in Desch (2015)) predicts a very icy Charon, contrary to observations. Of course, the model has adjustable parameters (rock density, ejected fraction) that could allow it to be retuned to give Charon's true density, but without direct numerical simulation of impacts between such structurally unusual (density unstable) bodies, it is hard to know what the real outcome for would be. Such simulations would be valuable. Naively, though, it seems likely that any exterior small satellites formed from the collisional debris would heavily sample these primordial rock- and carbonaceous-matter-rich outer layers, as these layers are closest to the original bodies' free surfaces. As noted above, there is no evidence, either optical or spectral, that Pluto's small satellites compositionally resemble dark, primordial Kuiper belt material (or more specifically, those KBOs or Centaurs of sizes most comparable to Pluto's small satellites and for which albedos are known (generally <20% (Weaver et al., 2016)).

### 6.2. Pebble accretion

The iciness of the small satellites is also not consistent with direct formation of the Pluto–Charon system from a streaming instability in the solar nebula followed by prompt collapse of gravitationally bound clumps of "pebbles" (Johansen et al., 2014), a proposed formation mechanism for Kuiper belt binaries, including Pluto–Charon (Nesvorný et al., 2010). A straightforward reading of the streaming instability/pebble-pile scenario predicts a primordial, or at least uniform, composition for all bodies in the system. That is, forming from the same cloud of collapsing pebbles and nebular gas, Pluto and Charon should have the same rock/ice ratio and the small satellites should be primordial in composition, which the latter show no indication of being. We note that Pluto and Charon have evolved in different ways, with Pluto having retained surface volatile ices and Charon likely having lost them due to the latter's lower gravity (Schaller and Brown, 2007), but this has already been addressed above in the  $m_3$  estimates for each.<sup>2</sup>

<sup>1</sup> The equivalent spherical radii of Nix and Hydra from Weaver et al. (2016), 19 and 21 km, respectively, are both smaller than the lower size limits given in Brozović et al. (2015). The small satellites turned out to have higher visual geometric albedos and smaller sizes than expected. This means, however, that the present upper limits on their bulk densities are large, greater the mean density of Pluto–Charon.

<sup>2</sup> The presence of NH<sub>3</sub> on Charon, Nix, and Hydra, as opposed to N<sub>2</sub> on Pluto, is a possible additional constraint, but different explanations exist (e.g., Cruikshank et al., 2016).

The above conclusion does not, however, rule out streaming instability and pebble accretion as a process in the ancestral Kuiper belt. Planetesimals much smaller than either Pluto or Charon (say, 50-to-100 km in diameter) can form directly in this manner, and they can grow, independently, to proto-Pluto (or proto-Charon) size through either traditional planetesimal collisions or further accretion of pebbles (Johansen et al., 2015). What is apparently ruled out is prompt formation of the entire Pluto–Charon system through the streaming instability and gravitational collapse of a massive pebble pile. This inference will be further tested when more precise, dynamically based densities are available for Nix and Hydra: if they are indeed ice in bulk, they should have densities under  $1 \text{ g/cm}^3$  due to porosity (similar densities to Saturn’s inner satellites).

### 6.3. Thermal considerations

We can draw further implications. That successful Pluto system formation models involve only partially differentiated precursors implies they could not have become so hot as to melt much of their ices and initiate full rock-from-ice differentiation before the Charon-forming impact. This implies that they must have accreted relatively late to limit  $^{26}\text{Al}$  and  $^{60}\text{Fe}$  heating, i.e., at least a few million years after the beginning of the Solar System, measured from the first condensation of calcium-aluminum inclusions ( $t_{\text{CAI}}$ ) (e.g., Merk and Prialnik, 2006; and see McKinnon et al., 2008). This constraint appears consistent with recent coagulation accretion models in the outer ancestral Kuiper belt ( $\sim 22$ -to- $27 \text{ AU}$ ) (i.e., Kenyon et al., 2008; Kenyon & Bromley 2012), which have Pluto-scale bodies taking more than 10 Myr to accrete (i.e., after solar nebula dispersal).

On the other hand, the timing of growth to 1000-km radius at 25 AU in some of the pebble accretion models in Johansen et al. (2015) is as short as 2 million years (after  $t_{\text{CAI}}$ ), which may be problematic, especially for  $^{60}\text{Fe}$  (half-life =  $2.4 \text{ m.y.}$ ; Tang and Dauphas, 2012). The low initial solar system abundance of  $^{60}\text{Fe}/^{56}\text{Fe}$  documented in Tang and Dauphas (2012) implies, however, that  $^{60}\text{Fe}$  decay was not an important heat source for bodies in the ancestral Kuiper belt (or elsewhere in the Solar System). If so, radiogenic heating in the early solar system by short-lived radionuclides was essentially entirely due to  $^{26}\text{Al}$ , which should have been at or close to its canonical abundance value in the outer protoplanetary disk (Larsen et al., 2016).

Accretion must also be slow enough so as to not bury the heat of accretion. How slow depends on how large the planetesimals (or pebbles) are. McKinnon et al. (2008) derive the following for the effective surface thermal conduction length during accretion:

$$\frac{\kappa}{u_{\text{acc}}} \sim 10 \text{ m} \times \left( \frac{1000 \text{ km}}{R_{\text{final}}} \right) \times \left( \frac{\tau_{\text{accretion}}}{10^6 \text{ yr}} \right), \quad (1)$$

where  $\kappa$  is the thermal diffusivity (assumed to be that of porous ice-rock) and  $u_{\text{acc}}$  is the radial rate of growth of the body. For impacts much larger than this scale, impact heat is effectively buried. Eq. (1) implies, even for long accretion times ( $\tau_{\text{accretion}}$ ), that traditional planetesimal sizes may be too large for impact heat to be efficiently radiated away during accretion. On the other hand, small-scale, pebble accretion would appear to be ideal for depositing accretional energy right at the surface, where it can be efficiently radiated away or advected away by nebular gas as a body accretes.

### 6.4. Challenges posed by Pluto’s small satellites

Two major unsolved origins problems remain for the small satellites. First, the numerical simulations in Canup (2011) generally result in more compact debris disks than the current positions of Styx, Nix, Kerberos, and Hydra. Most disk material was

presumably accreted by Charon, with only a very small fraction captured into resonances that would protect such from collision with Charon as the large moon tidally evolved outward from Pluto (Dobrovolskis et al., 1997). How this occurred exactly is an unsolved problem (see the extensive discussion in Peale and Canup (2015)), though Kenyon and Bromley (2014) and Bromley and Kenyon (2015) have presented a detailed model of how a viscously spreading ring or disk may expand out to the position of Hydra, and how circumbinary satellites may accrete near resonances. Walsh and Levison (2015) incorporated collisional evolution into such evolving disks or rings, including the impact disruption of earlier small satellites, and in contrast did not find preference for accretion near mean-motion resonances. As they note, Pluto’s small satellite system remains mysterious.

One prediction Kenyon and Bromley (2014) did make was that an ensemble of small moons (diameters  $\leq 2$ – $6 \text{ km}$ ), from the spreading debris disk, should presently still exist outside Hydra’s orbit. No moons larger than 1.7-km in diameter (for a Nix-like albedo of 0.5) have been found by New Horizons, however (Weaver et al., 2016). These overlapping limits do not disprove the spreading ring or disk concept, but the lack of any detected small satellites outside Hydra’s orbit, or even a diffuse dust ring in forward scattering, is not encouraging.

We note that Weaver et al. (2016) find from the shapes of Hydra and Kerberos that they appear to be structurally composite bodies, in the manner of many comets (e.g., Rickman et al., 2015). Kerberos appears to have two distinct lobes, whereas Hydra may have 2 or more. This could be taken to be the signature of the accretion process of these moons, in which ancestral moons on crossing orbits collided and merged. Their mean orbital speeds at present are in the range of  $\sim 120$ -to- $150 \text{ m/s}$ , so collision speeds for excited eccentricities of 0.1–0.2 may only be  $\sim 10$ – $30 \text{ m/s}$ . Even considering the modestly higher velocities for closer circumbinary orbits, such collision speeds would not have been destructive. The four satellites we see today are not likely to be the original set of satellites that accreted out of the post-impact debris disk (Walsh and Levison, 2015). There were likely many more small satellites, and Nix and Hydra (the largest) may have grown at the expense of former, smaller moons.

The second unsolved origins problem concerns the survival of the small satellites during the Nice (or a Nice-like) instability. If the Charon-forming impact occurred in the ancestral Kuiper belt, before the instability, which is strongly indicated by the low impact speeds required of the collision, then there is sufficient time for Charon’s orbital migration and that of the small satellites (Dobrovolskis et al., 1997; Cheng et al., 2014; Walsh and Levison, 2015), if the timing of the instability is taken to be coincident with the Late Heavy Bombardment ( $\sim 3.85$  billion years ago) (Gomes et al., 2005). Now, the Nice (or a related) dynamical instability could have occurred much earlier, before Charon completed its orbital evolution, and perhaps before the present small satellites formed or reached their present orbital distances from Pluto. But for the “nominal” case of a relatively late Nice-like instability, how stable are the distant, small satellite orbits and what is likelihood of survival of these satellites as Pluto is scattered outward into the Kuiper belt?

Pires et al. (2015) examined part of the small satellite survival problem dynamically, for the “nominal” case of a relatively late instability. They found that 84% of test Plutos placed into the 3:2 mean-motion resonance with Neptune, while the giant planets migrated outward, survive without losing their Nix and Hydra equivalents to close encounters with Neptune. These simulations only cover the endgame of Neptune’s Nice-model evolution, however, not the initial, most chaotic part, and do not simulate interaction of Pluto-like resonant bodies with the broader scattering population. In particular, the test Plutos are already in the 3:2 resonance,

and so are more-or-less protected from close Neptune encounters. Thus, in our view further work is needed to assess the orbital stability and likelihood of survival of Nix and Hydra during any Nice-like planetary rearrangement.

### 6.5. Implications for the Earth

Finally, we end this section on a speculative note: Earth's lost satellites. Given the evidence from Pluto, it seems quite likely the giant impact that formed the Earth's Moon also resulted in an external debris disk or ring. Most of this material should have been accreted to the Moon, either promptly or as the Moon tidally evolved outward. The debris disk itself may have spread outward, however, and if the terrestrial equivalents to Pluto's small moons formed, they could have been driven outward in resonance with the Moon. Today, the terrestrial equivalents to Styx, Nix, Kerberos, and Hydra, at similar same near-resonant positions, would all lie beyond 800,000 km from the Earth, or at greater than half a Hill radius. As such they would not be stable over the age of the Solar System (Murray and Dermott, 1999), and were likely lost to heliocentric orbit (after which they were either reaccreted or scattered).

## 7. Outlook

The New Horizons encounter with the Pluto system has finally resolved the long-standing issue (since 1930!) of Pluto's true size and density. With such data in hand for Pluto and Charon, and hopefully for Nix and Hydra in the not too distant future, newer and more precise models of Pluto and Charon's internal structure and evolution as well as the formation of the system, presumably by giant impact, can be developed and explored. The structural models presented in this paper are a small step in this direction. Precision does not confer accuracy, however. We do not (yet) know the presence or extent of oceans within either Pluto or Charon; nor do we have much constraint on the carbonaceous component within either body. Future work, say, on the excavation of the Sputnik Planitia basin by large-body impact (e.g., (Nimmo et al., 2016)), and of course, on the giant impact formation of Pluto–Charon, should be clarifying. Much remains to be done in terms of compositional, geological, and geophysical interpretation of existing New Horizons data as well. Ultimately, though, an accurate picture of the interiors of Pluto and Charon will only be achieved with newer sorts of data, such as global spectral imaging, radar sounding and gravity measurements, which can only be obtained by an orbiter mission.

### Acknowledgment

This research was supported by the New Horizons project, and NASA Planetary Geology and Geophysics Program grant NNX11AP16G. We thank the reviewers for their perceptive comments, but most of all we thank all those who have supported exploration of Pluto and the deep Outer Solar System over these many years.

### Appendix

#### Updated solar composition rock

Rather than simply adjust the PF mineralogy in Mueller and McKinnon (1988) to reflect new abundance values, we recalculate modal mineralogies based on the abundances in Lodders (2003). This eliminates any uncertainties in the original abundance values of Prinn and Fegley (1989), and facilitates direct comparisons to alternative mineralogies. The important global assumption is that the rock component is (or originally was) solar in bulk. Nominally it retains the full solar complement of iron and sulfur. We adopt

the condensation mineralogy in Prinn and Fegley (1982), in order of decreasing abundance: serpentine, troilite, tremolite, magnetite, “feldspar plus nepheline,” millerite, and anorthite. For serpentine we use antigorite, the high-pressure stable form, and for “feldspar plus nepheline” we specify nepheline. With this choice of 7 minerals one can constrain 7 elements, Mg, Fe, S, Al, Ca, Na, and Ni, to their Si-normalized CI abundances (NCFMASNiSu system).

The mineralogy is determined as follows: (1) the Ni abundance determines the millerite abundance; (2) the remaining S goes into troilite, with Fe remaining; (3) the Na abundance determines the nepheline abundance; (4) the remaining Al determines the anorthite abundance; (5) the remaining Ca from step 4 determines the tremolite abundance; (6) the remaining Mg and Si from steps 3–5, plus a portion of the remaining Fe, are used to make antigorite; and (7) leftover Fe goes to magnetite. This PF2-rock mineralogy is itemized in Table 1, along with the original PF-rock mineralogy from Mueller and McKinnon (1988), for comparison.

The STP density of this revised chondritic mineralogy is 3142 kg m<sup>-3</sup>, 3% less than the STP-density of PF-rock in Mueller and McKinnon (1988). About half of this modest difference is due to the updated solar abundances; the other half stems from a different serpentine density model (Mueller and McKinnon (1988) assumed lizardite as the polymorph). Serpentine dominates the mineralogy of both PF and PF2 rock, PF2 rock even more so. Overall, however, the stability of the mean density implies that future abundance revisions are unlikely to have much additional effect for the same mineralogical model.

New solar photospheric and CI chondrite meteoritic abundances continue to be made, and are summarized in the recent review of Palme et al. (2014). With regard to CI abundance values, which for rock-forming elements are inevitably more precise than photospheric determinations, the abundances of 6 of the 7 rock-forming elements above either have not changed or are within 0.01 dex ( $\approx 2\%$ ) of the recommended values in Lodders (2003), which were themselves created from a combination of photospheric and weighted CI abundances. Only calcium shows a greater shift,  $-0.03$  dex ( $\approx -7\%$ ), but the stated meteoritic uncertainty is also 0.03 dex, which covers the original value in Lodders (2003). Hence we do not consider it useful to generate a further update to the PF-rock model.

## References

- A'Hearn, M.F., et al., 2012. Cometary volatiles and the origin of comets. *Astrophys. J.* 758 (29), 8 pp. doi:10.1088/0004-637X/758/1/29.
- Airieu, S.A., Farquhar, J., Thiemens, M.H., Leshin, L.A., Bao, H., Young, E., 2005. Planetsimal sulfate and aqueous alteration in CM and CI carbonaceous chondrites. *Geochim. Cosmochim. Acta* 69, 4167–4172.
- Anders, E., Ebihara, M., 1982. Solar system abundances of the elements. *Geochim. Cosmochim. Acta* 46, 2363–2380.
- Anders, E., Grevesse, N., 1989. Abundances of the elements—meteoritic and solar. *Geochim. Cosmochim. Acta* 53, 197–214.
- Anthony, J.A., Bideaux, R.A., Bladh, K.W., Nichols, M.C., 1990. *Handbook of Mineralogy. Elements, Sulfides, Sulfosalts*, vol. 1. Mineral Data Publishing, Tucson.
- Asplund, M., Grevesse, N., Sauval, A.J., Scott, P., 2009. The chemical composition of the Sun. *Annu. Rev. Astron. Astrophys.* 47, 487–522. doi:10.1146/annurev.astro.46.060407.145222.
- Bagenal, F., et al., 2016. Pluto's interaction with its space environment: solar wind, energetic particles, and dust. *Science* 351. doi:10.1126/science.aad9045.
- Barr, A.C., Schwamb, M.E., 2016. Interpreting the densities of the Kuiper belt's dwarf planets. *Mon. Not. Royal Astron. Soc.* 460, 1542–1548. doi:10.1093/mnras/stw1052.
- Beyer, R.A., Nimmo, F., McKinnon, W.B., Moore, J.M., et al., 2016. Charon tectonics. Submitted to *Icarus*.
- Besserer, J., Nimmo, F., Roberts, J.H., Pappalardo, R.T., 2013. Convection-driven compaction as a possible origin of Enceladus's long wavelength topography. *J. Geophys. Res. Planets* 118, 908–915. doi:10.1002/jgre.20079.
- Bjerner, C.J., Nimmo, F., McKinnon, W.B., 2016. Testing for a compositional difference between Pluto and Charon. In: 47th Lunar Planet. Sci. Conference abs. #2176.
- Bockelée-Morvan, D., Crovisier, J., Mumma, M.J., Weaver, H.A., 2004. The composition of cometary volatiles. In: Festou, M.C., et al. (Eds.), *Comets II*. Univ. of Arizona Press, Tucson, pp. 391–423.

- Britt, D.T., Consolmagno, G.J., 2000. The porosity of dark meteorites and the structure of low-albedo asteroids. *Icarus* 146, 213–219.
- Bromley, B.C., Kenyon, S.J., 2015. Evolution of a ring around the Pluto–Charon binary. *Astrophys. J.* 809 (88), 19pp. doi:10.1088/0004-637X/809/1/88.
- Brown, M.E., 2008. The largest Kuiper belt objects. In: Barucci, M.A., Boehnhardt, H., Cruikshank, D., Morbidelli, A. (Eds.), *The Solar System beyond Neptune*. Univ. of Arizona Press, Tucson, pp. 335–344.
- Brown, M.E., 2012. The compositions of Kuiper belt objects. *Annu. Rev. Earth Planet. Sci.* 40, 467–494.
- Brown, M.E., 2013. The density of mid-sized Kuiper belt object 2002 UX25 and the formation of the dwarf planets. *Astrophys. J. Lett.* 778 (L34), 5.
- Brown, P.G., et al., 2001. The fall, recovery, orbit, and composition of the Tagish Lake meteorite: a new type of carbonaceous chondrite. *Science* 290, 320–325.
- Brownlee, D., 2014. The Stardust mission: analyzing samples from the edge of the Solar System. *Annu. Rev. Earth Planet. Sci.* 42, 179–205.
- Brozović, M., Showalter, M., Jacobson, R.A., Buie, M., 2015. The orbits and masses of satellites of Pluto. *Icarus* 246, 317–329. doi:10.1016/j.icarus.2014.03.015.
- Canup, R.M., 2005. A giant impact origin of Pluto–Charon. *Science* 307, 546–550.
- Canup, R.M., 2011. On a giant impact origin of Charon, Nix, and Hydra. *Astron. J.* 141, 35–44.
- Capaccioni, F., et al., 2015. The organic-rich surface of comet 67P/Churyumov-Gerasimenko as seen by VIRTIS/Rosetta. *Science* 347. doi:10.1126/science.aaa0628.
- Cheng, W.H., Lee, M.H., Peale, S.J., 2014. Complete tidal evolution of Pluto–Charon. *Icarus* 233, 242–258.
- Consolmagno, G.J., Britt, D.T., Macke, R.J., 2008. The significance of meteorite density and porosity. *Chemie der Erde – Geochem* 68, 1–29. doi:10.1016/j.chemer.2008.01.003.
- Cook, J.C., et al., 2016. Spectroscopy of Pluto's small satellites. In: *Division for Planetary Sciences 48/European Planetary Science Conference 11 abs. #205.05*.
- Crovisier, J., Biver, N., Bockelée-Morvan, D., Colom, P., 2009. Radio observations of Jupiter-family comets. *Planet. Space Sci.* 57, 1162–1174.
- Cruikshank, D.P., et al., 2016. Pluto and Charon: surface colors and compositions—A hypothesis. In: *47th Lunar Planet. Sci. Conference abs. #1696*.
- Davidsson, B.J.R., et al., 2016. The primordial nucleus of comet 67P/Churyumov-Gerasimenko. *Astron. Astrophys.* 592, A63. doi:10.1051/0004-6361/201526968.
- Desch, S.J., 2015. Density of Charon formed from a disk generated by the impact of partially differentiated precursors. *Icarus* 246, 37–47. doi:10.1016/j.icarus.2014.07.034.
- Dobrovolskis, A.R., Peale, S.J., Harris, A.W., 1997. Dynamics of the Pluto–Charon binary. In: Stern, S.A., Tholen, D.J. (Eds.), *Pluto and Charon*. Univ. of Arizona Press, Tucson, pp. 159–190.
- Durham, W.B., McKinnon, W.B., Stern, L.A., 2005. Cold compaction of water ice. *Geophys. Res. Lett.* 32, L18202. doi:10.1029/2005GL023484.
- Festou, M.C., Keller, H.U., Weaver, H.A., 2004. *Comets II*. University of Arizona Press, Tucson.
- Fink, U., 2009. A taxonomic survey of comet composition 1985–2004 using CCD spectroscopy. *Icarus* 201, 311–334.
- Fomenkova, M.N., 1999. On the organic refractory component of cometary dust. *Space Sci. Rev.* 90, 109–114.
- Fray, N., et al., 2016. High-molecular-weight organic matter in the particles of comet 67P/Churyumov-Gerasimenko. *Nature* 538, 72–74. doi:10.1038/nature19320.
- Fulle, M., et al., 2016. Comet 67P/Churyumov-Gerasimenko preserved the pebbles that formed planetesimals. *Mon. Not. Royal Astron. Soc.* 462 (Suppl. 1), s132–s137. doi:10.1093/mnras/stw2299.
- Gladstone, G.R., et al., 2016. The atmosphere of Pluto as observed by New Horizons. *Science* 351. doi:10.1126/science.aad8866.
- Goesmann, F., et al., 2015. Organic compounds on comet 67P/Churyumov-Gerasimenko revealed by COSAC mass spectrometry. *Science* 349. doi:10.1126/science.aab0689.
- Gomes, R., Levison, H.F., Tsiganis, K., Morbidelli, A., 2005. Origin of the cataclysmic Late Heavy Bombardment period of the terrestrial planets. *Nature* 435, 466–469.
- Gounelle, M., Zolensky, M.E., 2001. A terrestrial origin for sulfate veins in CI1 chondrites. *Meteor. Planet. Sci.* 36, 1321–1329.
- Grundy, W.M., Porter, S.B., Benecchi, S.D., Roe, H.G., Noll, K.S., Trujillo, C.A., Thirouin, A., Stansberry, J.A., Barker, E., Levison, H.F., 2015. The mutual orbit, mass, and density of the large transneptunian binary system Varda and Ilmarë. *Icarus* 257, 130–138. doi:10.1016/j.icarus.2015.04.036.
- Grundy, W.M., et al., 2016. Surface compositions across Pluto and Charon. *Science* 351. doi:10.1126/science.aad9189.
- Greenstreet, S., Gladman, B., McKinnon, W.B., 2015. Impact and cratering rates onto Pluto. *Icarus* 258, 267–288. doi:10.1016/j.icarus.2015.05.026.
- Hammond, N.P., Barr, A.C., Parmentier, E.M., 2016. Recent tectonic activity on Pluto driven by phase changes in the ice shell. *Geophys. Res. Lett.* 43. doi:10.1002/2016GL069220.
- Hartogh, P., et al., 2011. Ocean-like water in the Jupiter-family comet 103P/Hartley 2. *Nature* 478, 218–220.
- Housen, K.R., Holsapple, K.A., 2011. Ejecta from impact craters. *Icarus* 211, 856–875. doi:10.1016/j.icarus.2010.09.017.
- Hussmann, H., Sohl, F., Spohn, T., 2006. Subsurface oceans and deep interiors of medium-sized outer planet satellites and large trans-neptunian objects. *Icarus* 185, 258–273.
- Jessberger, E.K., Christoforidis, A., Kissel, J., 1988. Aspects of the major element composition of Halley's dust. *Nature* 332, 691–695.
- Johansen, A., Blum, J., Tanaka, H., et al., 2014. The multifaceted planetesimal formation process. In: Beuther, H., Klessen, R.S., Dullemond, C.P., Henning, T. (Eds.), *Protostars and Planets VI*. University of Arizona Press, Tucson, pp. 547–570.
- Johansen, A., Mac Low, M.-M., Lacerda, P., Bizzarro, M., 2015. Growth of asteroids, planetary embryos, and Kuiper belt objects by chondrule accretion. *Sci. Adv.* 1 11pp, e1500109.
- Kenyon, S.J., Bromley, B.C., 2012. Coagulation calculations of icy planet formation at 15–150 AU: a correlation between the maximum radius and the slope of the size distribution for transneptunian objects. *Astron. J.* 143 21pp.
- Kenyon, S.C., Bromley, B.C., 2014. Formation of Pluto's low-mass satellites. *Astron. J.* 147 (8), 17pp. doi:10.1088/0004-6256/147/1/8.
- Kenyon, S.C., Bromley, B.C., O'Brien, D.P., Davis, D.R., 2008. Formation and collisional evolution of Kuiper belt objects. In: Barucci, M.A., Boehnhardt, H., Cruikshank, D., Morbidelli, A. (Eds.), *The Solar System beyond Neptune*. Univ. of Arizona Press, Tucson, pp. 293–313.
- Kofman, W., et al., 2015. Properties of the 67P/Churyumov-Gerasimenko interior revealed by CONSERT radar. *Science* 349. doi:10.1126/science.aab0639.
- Küppers, M., et al., 2005. A large dust/ice ratio in the nucleus of comet 9P/Tempel 1. *Nature* 437, 987–990. doi:10.1038/nature04236.
- Larsen, K.K., Schiller, M., Bizzarro, M., 2016. Accretion timescales and style of asteroidal differentiation in an <sup>26</sup>Al-poor protoplanetary disk. *Geochim. Cosmochim. Acta* 176, 295–315. doi:10.1016/j.gca.2015.10.036.
- Levison, H.F., Morbidelli, A., VanLaerhoven, C., Gomes, R., Tsiganis, K., 2008. Origin of the structure of the Kuiper belt during a dynamical instability in the orbits of Uranus and Neptune. *Icarus* 196, 258–273.
- Levison, H.F., Morbidelli, A., Tsiganis, K., Nesvorný, D., Gomes, R., 2011. Late orbital instabilities in the outer planets induced by interaction with a self-gravitating planetesimal disk. *Astrophys. J.* 142, 152.
- Lisse, C.M., Kraemer, K.E., Nuth, J.A., Li, A., Joswiak, D., 2007. Comparison of the composition of the Tempel 1 ejecta to the dust in Comet C/Hale-Bopp 1995 O1 and YSO HD 100546. *Icarus* 187, 69–86.
- Lockwood, A.C., Brown, M.E., Stansberry, J., 2014. The size and shape of the oblong dwarf planet Haumea. *Earth Moon Planet* 111, 127–137. doi:10.1007/s11038-014-9430-1.
- Lodders, K., 2003. Solar system abundances and condensation temperatures of the elements. *Astrophys. J.* 591, 1220–1247.
- Lodders, K., Palme, H., Gail, H.P., 2009. *Abundances of the elements in the solar system*. In: Trumpler, J.E. (Ed.), *Landolt-Bornstein, New Series*, vol. VI/4B. Springer-Verlag, Berlin, pp. 560–630.
- Macke, R.J., Consolmagno, G.J., Britt, D.T., 2011. Density, porosity, and magnetic susceptibility of carbonaceous chondrites. *Meteor. Planet. Sci.* 46, 1842–1862. doi:10.1111/j.1945-5100.2011.01298.x.
- Malamud, U., Prialnik, D., 2015. Modeling Kuiper belt objects Charon, Orcus and Salacia by means of a new equation of state for porous icy bodies. *Icarus* 246, 21–36. doi:10.1016/j.icarus.2014.02.027.
- McKinnon, W.B., 1984. On the origin of Triton and Pluto. *Nature* 311, 355–358. doi:10.1038/311355a0.
- McKinnon, W.B., 1989. On the origin of the Pluto–Charon binary. *Astrophys. J.* 344, L41–L44 (Erratum: *Astrophys. J. Lett.* 346, L106).
- McKinnon, W.B., Bland, M.T., 2011. Core evolution in icy satellites and Kuiper belt objects. In: *42nd Lunar and Planetary Science Conference abs. #2768*.
- McKinnon, W.B., Mueller, S., 1988. Pluto's structure and composition suggest origin in the solar, not a planetary, nebula. *Nature* 335, 240–243.
- McKinnon, W.B., Lunine, J.I., Banfield, D., 1995. Origin and evolution of Triton. In: Cruikshank, D.P. (Ed.), *Neptune and Triton*. University of Arizona Press, Tucson, pp. 807–877.
- McKinnon, W.B., Simonelli, D.P., Schubert, G., 1997. Composition, internal structure, and thermal evolution of Pluto and Charon. In: Stern, S.A., Tholen, D.J. (Eds.), *Pluto and Charon*. Univ. of Arizona Press, Tucson, pp. 295–343.
- McKinnon, W.B., Prialnik, D., Stern, S.A., Coradini, A., 2008. Structure and evolution of Kuiper belt objects and dwarf planets. In: Barucci, M.A., Boehnhardt, H., Cruikshank, D., Morbidelli, A. (Eds.), *The Solar System beyond Neptune*. Univ. of Arizona Press, Tucson, pp. 213–241.
- McKinnon, W., et al., 2014. Cosmogonic constraints from densities in the Pluto system and rotational and tidal figures of equilibrium for Pluto and Charon. In: Muinonen, K., et al. (Eds.), *Proc. Asteroids, Comets, Meteors 2014*, Helsinki, Finland, p. 346.
- McKinnon, W.B., Nimmo, F., Wong, T., Schenk, P.M., White, O.L., Roberts, J.H., Moore, J.M., Spencer, J.R., Howard, A.D., Umurhan, O.M., Stern, S.A., Weaver, H.A., Olkin, C.B., Young, L.A., Ennico Smith, K., the New Horizons Geology, Geophysics and Imaging Theme Team, 2016. Convection in a volatile nitrogen-ice-rich layer drives Pluto's geological vigour. *Nature* 534, 82–85. doi:10.1038/nature18289.
- Merk, R., Prialnik, D., 2006. Combined modeling of thermal evolution and accretion of trans-neptunian objects: occurrence of high temperatures and liquid water. *Icarus* 183, 283–295.
- Morbidelli, A., Levison, H.F., Gomes, R., 2008. The dynamical structure of the Kuiper belt and its primordial origin. In: Barucci, M.A., Boehnhardt, H., Cruikshank, D., Morbidelli, A. (Eds.), *The Solar System beyond Neptune*. Univ. of Arizona Press, Tucson, pp. 275–292.
- Mueller, S., McKinnon, W.B., 1988. Three-layered models of Ganymede and Callisto: Compositions, structures, and aspects of evolution. *Icarus* 76, 437–464.
- Moore, J.M., Howard, A.D., Schenk, P.M., McKinnon, W.B., et al., 2015. Geology before Pluto: pre-encounter considerations. *Icarus* 246, 65–81. doi:10.1016/j.icarus.2014.04.028.

- Moore, J.M., et al., 2016. The geology of Pluto and Charon through the eyes of new horizons. *Science* 351, 1284–1293. doi:10.1126/science.aad8866.
- Mumma, M.J., Charnley, S.B., 2011. The chemical composition of comets—Emerging taxonomies and natal heritage. *Annu. Rev. Astron. Astrophys.* 49, 471–524.
- Murray, C.D., Dermott, S.F., 1999. *Solar System Dynamics*. Cambridge Univ. Press, Cambridge, U.K.
- Nesvorný, D., 2015a. Evidence for slow migration of Neptune from the inclination distribution of Kuiper belt objects. *Astron. J.* 150 (73), 18pp. doi:10.1088/0004-6256/150/3/73.
- Nesvorný, D., 2015b. Jumping Neptune can explain the Kuiper belt kernel. *Astron. J.* 150 (68), 14pp. doi:10.1088/0004-6256/150/3/68.
- Nesvorný, D., Morbidelli, A., 2012. Statistical study of the early solar system's instability with four, five, and six giant planets. *Astron. J.* 144 (117), 20pp. doi:10.1088/0004-6256/144/4/117.
- Nesvorný, D., Vokrouhlický, D., 2016. Neptune's orbital migration was grainy, not smooth. *Astrophys. J.* 825 (14). doi:10.3847/0004-637X/825/2/94.
- Nesvorný, D., Youdin, A.N., Richardson, D.C., 2010. Formation of Kuiper Belt binaries by gravitational collapse. *Astron. J.* 140, 785–793.
- Nimmo, F., Hamilton, D.P., McKinnon, W.B., et al., 2016. Reorientation of Sputnik Planitia implies a subsurface ocean on Pluto. *Nature*, in press. <http://dx.doi.org/10.1038/nature20148>.
- Nimmo, F., et al., 2017. Mean radius and shape of Pluto and Charon from *New Horizons* images. *Icarus*. doi:10.1016/j.icarus.2016.06.027.
- Palme, H., Lodders, K., Jones, A., 2014. Solar system abundances of the elements. In: Turekian, K. (Ed.), *Treatise on Geochemistry, Second ed., Vol. 2: Planets, Asteroids, Comets and the Solar System*. Elsevier, Amsterdam, pp. 15–36.
- Peale, S.J., Canup, R.M., 2015. The origin of the natural satellites. In: Schubert, G. (Ed.), *Treatise on Geophysics, Second ed., Vol. 10: Physics of Terrestrial Planets and Moons*. Elsevier, Amsterdam, pp. 559–604.
- Pires, P., Giulietti Winter, S.M., Gomes, R.S., 2015. The evolution of a Pluto-like system during the migration of the ice giants. *Icarus* 246, 330–338. doi:10.1016/j.icarus.2014.04.029.
- Prinn, R.G., Fegley, B., 1981. Kinetic inhibition of CO and N<sub>2</sub> reduction in circumplanetary nebulae: implications for satellite composition. *Astrophys. J.* 249, 308–317.
- Reuter, D.C., et al., 2008. Ralph: a visible/infrared imager for the *New Horizons* Pluto/Kuiper belt mission. *Space Sci. Rev.* 140, 129–154. doi:10.1007/s11214-008-9375-7.
- Rickman, H., et al., 2015. Comet 67P/Churyumov-Gerasimenko: constraints on its origin from OSIRIS observations. *Astron. Astrophys.* 583, A44. doi:10.1051/0004-6361/201526093.
- Robouchon, G., Nimmo, F., 2011. Thermal evolution of Pluto and implications for surface tectonics and a subsurface ocean. *Icarus* 216, 426–439.
- Rotundi, A., et al., 2015. Dust measurements in the coma of comet 67P/Churyumov-Gerasimenko inbound to the Sun. *Science* 347. doi:10.1126/science.aaa3905.
- Sandford, S., et al., 2006. Organics captured from Comet 81P/Wild 2 by the Stardust spacecraft. *Science* 341, 1720–1724.
- Schaller, E.L., Brown, M.E., 2007. Volatile loss and retention on Kuiper belt objects. *Astrophys. J.* 659, L61–L64.
- Sicardy, B., et al., 2011. A Pluto-like radius and a high albedo for the dwarf planet Eris from an occultation. *Nature* 478, 493–496. doi:10.1038/nature10550.
- Stern, S.A., Weaver, H.A., Steffl, A.J., et al., 2006. A giant impact origin for Pluto's small moons and satellite multiplicity in the Kuiper belt. *Nature* 439, 946–948.
- Stern, S.A., et al., 2015. The Pluto system: initial results from its exploration by *New Horizons*. *Science* 350. doi:10.1126/science.aad1815.
- Tang, H., Dauphas, N., 2012. Abundance, distribution, and origin of <sup>60</sup>Fe in the solar protoplanetary disk. *Earth Planet. Sci. Lett.* 359–360, 248–263. doi:10.1016/j.epsl.2012.10.011.
- Tsiganis, K., Gomes, R., Morbidelli, A., Levison, H.F., 2005. Origin of the orbital architecture of the giant planets of the Solar System. *Nature* 435, 459–461.
- Walsh, K.J., Levison, H.F., 2015. Formation and evolution of Pluto's small satellites. *Astron. J.* 150 (11), 12pp. doi:10.1088/0004-637X/809/1/88.
- Weaver, H.A., et al., 2016. The small satellites of Pluto as observed by *New Horizons*. *Science* 351. doi:10.1126/science.aae0030.
- Wieczorek, M.A., et al., 2013. The crust of the moon as seen by GRAIL. *Science* 339, 671–675.
- Zolensky, M.E., Nakamura, K., Gounelle, M., Mikouchi, T., Kasama, T., Tachikawa, O., Tono, E., 2002. Mineralogy of Tagish Lake: a grouped type 2 carbonaceous chondrite. *Meteor. Planet. Sci.* 37, 737–761.
- Zolotov, M.Yu., 2009. On the composition and differentiation of Ceres. *Icarus* 204, 183–193. doi:10.1016/j.icarus.2009.06.011.